Electrochemical synthesis of Co_7Ni_3 and Co_6Ni_4 nanorods with controlled crystalline phase. Application to methanol electro-oxidation

Joan Vilana, Daniel Escalera-López, Elvira Gómez, Elisa Vallés*

Ge-CPN, Departament de Química Física and Institut de Nanociència i Nanotecnologia (IN^2UB), Universitat de Barcelona, Martí i Franquès 1, 08028 Barcelona, Spain.

*Author to whom correspondence should be addressed
e-mail: e.valles@ub.edu
Phone: +34 934039238
Fax: +34 934021231

Abstract

The conditions to synthesise, from a single solution, CoNi nanorods with modulated crystalline structure have been defined. The growth of the nanorods in the interior on the nanochannels of the membrane is mainly controlled by the limited transport of the Co(II) and Ni(II) ions to the growth front, but we have achieved the synthesis of micrometric CoNi nanorods with uniform crystalline structure and composition along the rod. Several microns CoNi nanorods showing similar composition but different phase as a function of the synthesis conditions have been obtained. The test of the two type of nanorods respect to methanol electro-oxidation demonstrated both the specific electrocatalytic behaviour of each one and the promising behaviour of the nanorods as electrocatalysts in direct methanol fuel cells in basic medium, due to their higher surface/volume ratio than that of thin films and the superior stability than that of nanoparticles. The influence of the crystalline structure in the methanol electro-oxidation has been also corroborated from pure-hcp and pure-fcc CoNi films.

Keywords: CoNi alloys, nanorods, nanofabrication, electrocatalytic behaviour, methanol electro-oxidation

1.-Introduction

The electrodeposition of CoNi alloys, by using different cobalt and nickel salts, concentrations, pH and electrochemical conditions, has been widely investigated, being the anomalous co-deposition mechanism well established [1-5]. Recently, the relationship between the composition, the morphology and the crystalline structure of thin films of CoNi and the electrochemical parameters of synthesis has been analysed [6-11], and the structural properties have been correlated with the corrosion or the tribological behaviour [12-14].

Also, the magnetic behaviour of the CoNi alloys has motivated the development of different electrochemical methods of synthesis of CoNi nanorods and nanowires using alumina or polycarbonate membranes as templates [15-19]. One side of the membranes is covered with a thin layer of metal, and the alloy is deposited from the electroactive species present in the solution through the pores of the membrane. The relationship between the properties of the nanorods and their magnetic properties has been investigated [20-24]. Lastly, in the last years, some research has been published about the possible use of CoNi alloys as catalysts [25] for hydrogen evolution [26-28] and for oxidation of methanol [29-31] or ethanol [32] in fuel cells, in order to replace noble metal catalysts due to their high cost. However, the possibility of using CoNi nanorods as catalysts for fuel cells applications has been not tested, because only CoNi films [30,31] or nanoparticles[29,32] have been tested. In order to study the applicability of 1D CoNi nanostructures, the challenge is the maintenance of the properties of the CoNi nanorods during their growth from the bottom to the end, especially for those of micrometric length. After the initial deposition on the metal seed layer at the bottom of the pores, the growth of the nanorods is limited by the partial depletion of the reducing species near the substrate and their mass transport through the channels of the pores, which controls the deposition rate [33-34]. The transport rate of the different reducing species can be different. This could induce the variation of the alloy composition and of the crystalline structure along the nanorods.

The aim of the present work is 1) defining the electrochemical synthesis conditions to obtain, from a single solution, CoNi nanorods of micrometric length and similar composition but different crystalline structure, maintaining both composition and crystalline structure from the initio of the deposition on the bottom of the pores to the final extreme of nanorods several microns long, and

2) testing the electrocatalytic behaviour of each type of nanorods for methanol electro-oxidation in basic medium. We select the CoNi system because although different authors have electrochemically synthesised CoNi of a specific composition using a defined solution, we have found that it is possible to synthesise CoNi nanorods and nanowires of different average composition and crystalline phase predominance, from a single solution, as a function of the deposition potential [16, 24]. The test of the influence of the crystalline structure of the electrocatalysts in methanol electro-oxidation for Direct Methanol Fuel Cells has been not before investigated. Some works are centred in analyse different CoNi alloy compositions in the catalysts performance [29-31]. In this work we try to prepare CoNi nanorods with different crystalline structure but with very similar composition. Previously to the study of the behaviour of the different nanorods prepared, we will analyse the effect of pure-hcp or pure-fcc CoNi films in the electrocatalytic process. Methanol is one of the most promising fuels for energy generation in fuel cells [30], and new CoNi micro/nanostructures can be promising catalysts of its electro-oxidation in basic medium, as effective platinum-free electrocatalysts. The nanowire structure is an interesting form for the catalysts in fuel cells due to their high area/volume ratio and higher stability than nanoparticles.

2.-Materials and methods

CoNi nanorods were electrochemically grown in the inner of track-edged polycarbonate membranes Isopore VCPT02500 0.1 μm (Millipore/Merk), 20 μm thick, with a nominal porosity of 4.18% and 100 nm of nominal pores diameter. To perform the electrochemical deposition, one of the sides of the membranes was coated, by means of a sputtering treatment, with a gold layer of around 100 nm to enable conductivity. Prior to electrodeposition, the membranes were kept in distilled water for several hours and afterwards in the CoNi solution to increase the hydrophilic behavior and the subsequent filling of the pores for the growth of the nanorods. The electrolytic bath consisted on a 0.2 M $CoCl_2$ + 0.9 M $NiCl_2$ + 0.5 M boric acid solution at pH=3, prepared using analytical grade reagents and Millipore Milli Q pure water. Oxygen was removed from the solution before the electrochemical experiments by argon bubbling and kept under positive argon pressure. Temperature during experiments was 20±2 ºC.

The electrochemical deposition was performed in a three-electrode custom-sized cell containing the coated membranes at the bottom as working electrode, a Ag/AgCl/KCl 3M (Metrohm) as reference electrode and a platinum spiral as auxiliary electrode. Before each electrochemical measurement the Pt electrode was annealed in a natural gas flame and quenched in ultrapure water for efficient

residue removal. A potentiostat/galvanostat Autolab with PGSTAT30 equipment and GPES software was used. The synthesis of the nanorods was performed in potentiostatic conditions (by applying potentials between -800 and -1000 mV). Nanorods length was controlled as a function of the circulated current density. In order to obtain pure-hcp and pure-fcc CoNi films, the deposition was performed on Si/Ti(50 nm)/Au(100 nm) plates, by applying different potentials and under convection conditions (100 r.p.m.)

The composition, length and crystalline structure of the nanorods was analysed after electrochemical preparation. The composition was determined by and X-ray Fluorescence Ficherscope system XDAL with WinFTM XDAL Ver6.19 software. A Hitachi H-4100FE (field emission SEM), Hitachi H800 MT and JEOL 2100 (TEM microscopes) were used for bright field observation and diffraction patterns analysis for crystalline structure determination.

The electrochemical study of the methanol oxidation was made in the three-electrode cell using solutions containing NaOH and methanol, with analytical grade reagents and Millipore Milli Q pure water. Counter and reference electrodes were the same that those previously described. As working electrodes, the synthesised CoNi deposits were used. In the case of the films, the Si/Ti/Au/CoNi substrates were directly used. In the case of the CoNi nanorods, these are placed on the surface of a glassy carbon electrode, of 2 mm of diameter.

3.-Results and discussion

3.1.-Synthesis of CoNi nanorods of micrometric length. Characterization

The CoNi nanorods were prepared in the interior of the polycarbonate membranes coated with gold layers. Potentiostatic deposition was performed, by applying different potentials in order to induce different growth rate of the alloy.

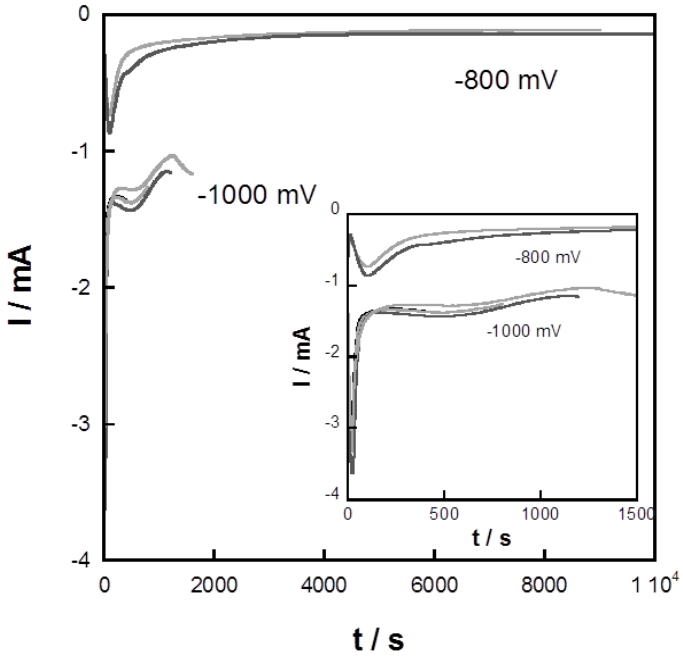

Figure 1

Figure 1 shows different chronoamperometric curves corresponding to the synthesis of CoNi nanorods at different times and two applied potentials. Long deposition times were used in order to grow long CoNi nanorods. The intensity clearly decreased (in absolute value) after the initial deposition, due to the depletion of the electroactive species (Co(II) and Ni(II)) on the surface of the electrode. Although stirring of the solution with argon flow near the membranes was used, the effect of the convection in the interior of the membrane's channels is null and the intensity attains an almost stationary value corresponding to the stationary transport regime of diffusion and migration of the electroactive species. The reproducible curves obtained at different deposition times demonstrate that the effective area for different coated membranes is very similar. By applying more negative potentials, the recorded current was obviously higher (more negative), as corresponds to higher deposition rate. The different values of the quasi stationary current detected at the different applied potentials are consequence of the different migration flux of the electroactive species as a function of the electric field.

The smooth maximum detected in the curves of -1000 mV at around 1200 s is assigned to the simultaneous hydrogen evolution on the CoNi formed, with gradual depletion of the protons. Simultaneous hydrogen evolution is favoured making the potential more negative.

Nanorods of different length were prepared in order to analyse the evolution of their average composition. Compact nanorods of uniform length were obtained for each deposition time at the two applied potentials (Figure 2). The nanorods length-time slope obviously increases for a more negative deposition potential, in according to a higher deposition rate.

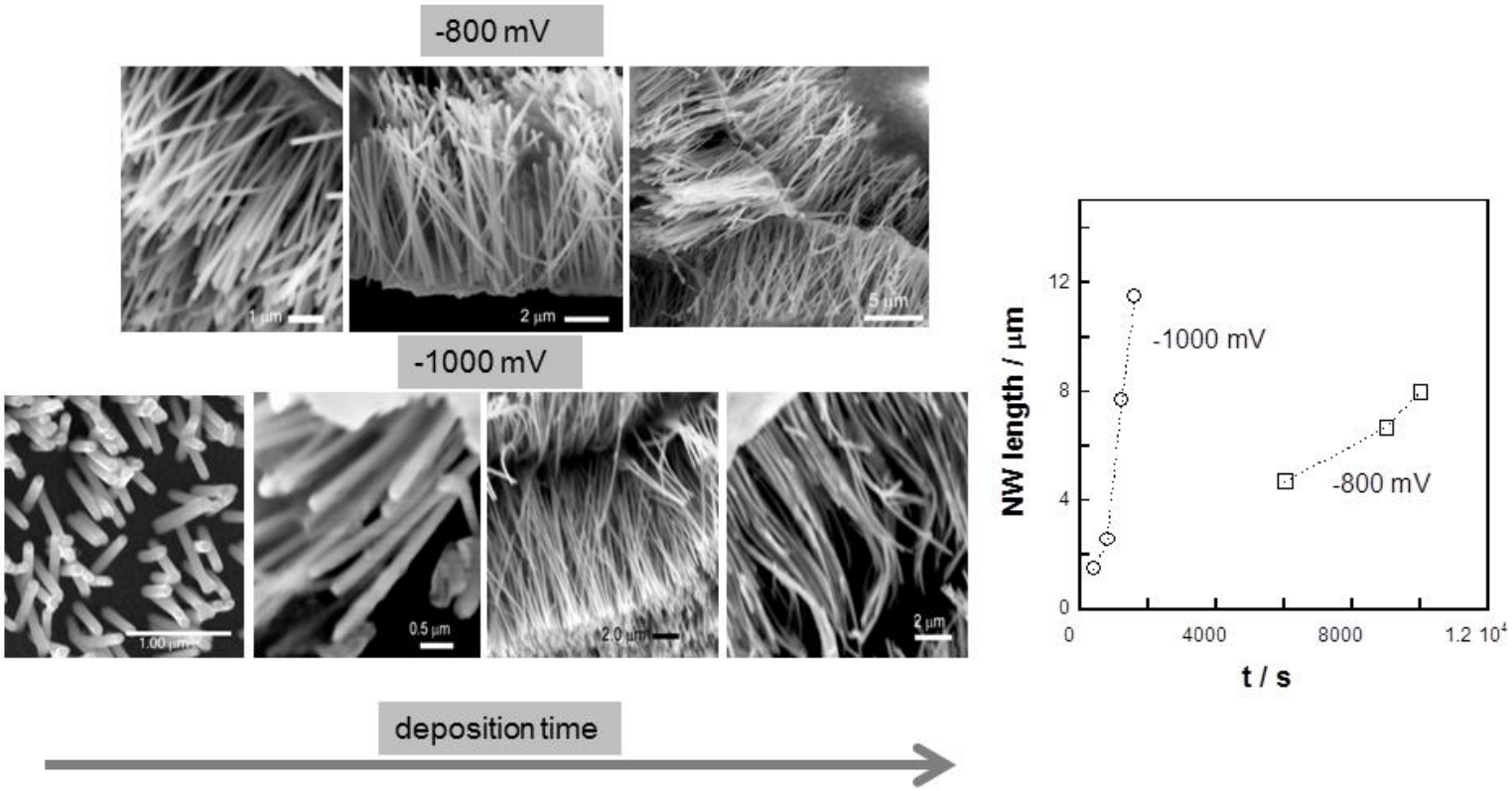

Figure 2

For each applied potential, no significant differences in composition were observed as a function of the length of the nanorods, which corroborates that the CoNi deposition process is controlled by the transport regime (low variation of the mobility and diffusion coefficient of the Ni(II) and Co(II) species with the potential, as the manner that the ratio of both species arriving to the growing nanorods will be approximately constant with the potential). The constancy of the composition of the nanorods: Co_7Ni_3 for those deposited at -800mV and Co_6Ni_4 for those synthesised at -1000 mV, regardless of the different deposition time demonstrates the uniformity of the nanorods during their growth. However, the growth rate of the nanorods was significantly different with the potential, as it is expected.

For a detailed observation of the nanorods and the analysis of the crystalline structure along them, the nanorods were released from the membranes, by etching with acetone or chloroform, and the gold seed layer was removed using a saturated KI_3 solution. The cleaned NWs are placed in a usual TEM copper grid. TEM images show well-built and compact nanorods at both deposition potentials, from the starting point, where a residual Au from membrane sputtering can be seen (Figure 3), in a form of small spherical drops at one end of wire allowing to know the part where start to grow.

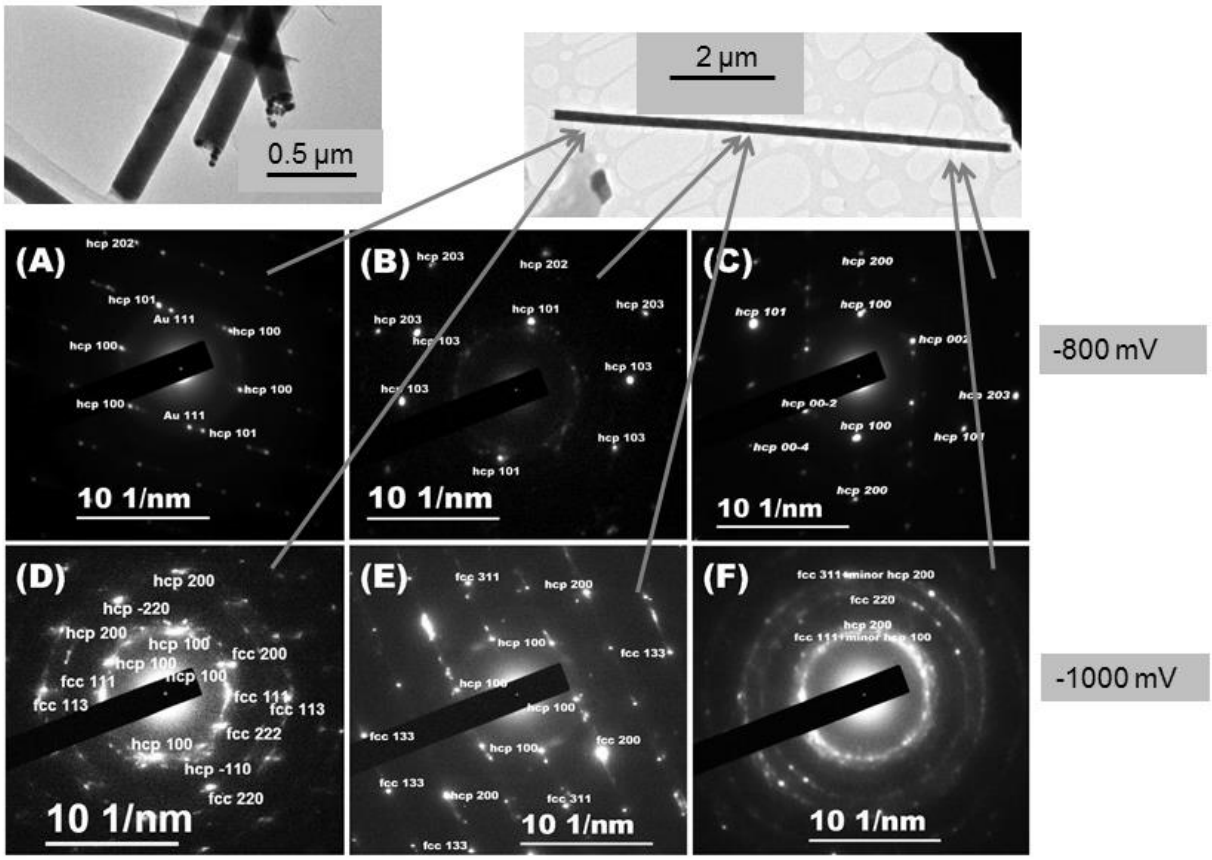

Figure 3

The crystalline structure of long nanorods (around 8-10 µm) was analysed from Selected Area Electron Diffraction (SAED) patterns taken at different distances from the bottom of the nanorods. Figure 3 shows representative images of the onset (A, D), middle (B, E) and final (C, F) parts of the CoNi nanorods. The main phase detected always for the nanowires prepared at low potential (-800 mV) is the hcp, as could be expected for the low growth rate, which favours the more stable crystalline structure of cobalt, the main component of the alloy, at room temperature. The c* axis of the hcp phase is not oriented parallel to the nanorods axis. However, the nanorods synthesised at

more negative potential (-1000 mV) correspond at a mixed hcp+fcc phase, from the bottom to the end. Although the composition of the nanorods is similar at the two potential of synthesis, the growth rate determines their crystalline structure. An increase of the deposition rate favours the formation of fcc phase and a more polycrystalline structure, reflected in the more defined diffraction rings in these conditions.

Therefore, constant properties (composition and crystalline structure) are observed along the long nanorods, which can condition the behaviour of them respect to their catalytic properties in methanol electro-oxidation.

3.2.-CoNi nanorods as catalysts in methanol electro-oxidation

From the previous study, CoNi nanorods of micrometric length (around 3 microns), synthesised at the two different potentials (-800 and -1000 mV), were tested as catalysts for methanol electro-oxidation in basic medium. In order to analyse their catalytic behaviour, pure hcp and fcc CoNi films have been tested as reference, because the influence of the crystalline structure of electrocatalysts of similar composition has not previously investigated. We prepared Co_7Ni_3 films of pure-hcp structure (at -800 mV) and Co_6Ni_4 films of pure-fcc structure (at -1000 mV), according to a previous study of the crystalline structure of CoNi films [24]. In the case of the CoNi deposits, it is possible to obtain films of pure fcc phase from the bath studied by applying enough negative potentials (-1000 mV), whereas the nanorods obtained at the same potential correspond, as it has been determined in the earlier section, to a hcp+fcc mixed phase, attributed to the lower deposition rate through the channels of the membrane.

The Figure 4 shows the morphology of the CoNi films synthesised at the different potentials, typical of an hcp cobalt phase (A) and an fcc CoNi phase (B). Figure 4 also shows the voltammetric curves recorded on the Si/Ti/Au/CoNi (1 µm thick) films, between 0 and 0.8 V at 50 mV s^{-1}, in a solution containing 0.5 M NaOH (or 0.5 M NaOH + 0.5 M methanol). The curves correspond to the steady profile obtained after successive cycling (30 cycles). The oxidation peak obtained in the NaOH solution, assigned to the $Ni(OH)_2 \rightarrow NiOOH$ process [31], appears at 350 mV for the hcp Co_7Ni_3 film, and at 275mV for the fcc Co_6Ni_4 film, which reveals that the fcc structure can be easily oxidised than the hcp. The peaks corresponding to the $CoO \leftrightarrow Co_2O_3$ redox couple are insignificant compared with the one corresponding to the $Ni(OH)_2 \leftrightarrow NiOOH$ redox couple. The current corresponding to the methanol electro-oxidation was detected at around 570 mV over the oxidized surface of the CoNi films.

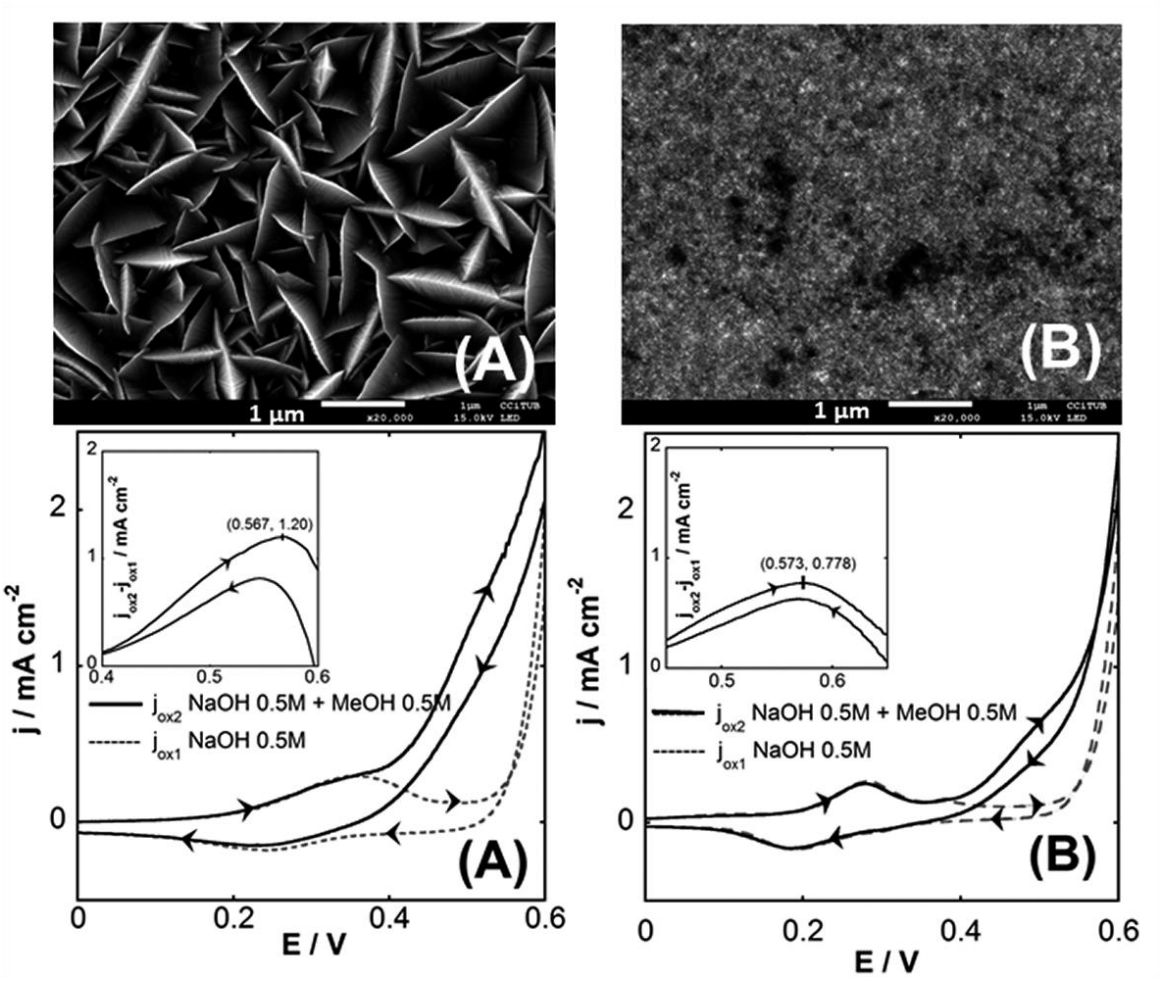

Figure 4

Although the composition of the two films is similar, the net peak corresponding to the methanol oxidation is higher in the case of the Co_7Ni_3 hcp film, unlike the reported in other papers [30,31]. As the current density was calculated using the geometrical area of the films, the better performance of Co_7Ni_3 could be attributed at the increase of effective area generated by the hcp morphology as suggested by other authors [31]. We can conclude that for similar compositions of the CoNi films, the crystalline structure, which conditions the morphology of the films, affects the performance of the CoNi catalysts for the methanol electro-oxidation.

The performance of CoNi nanorods of 2.75 µm, synthesised at the same potentials than the films, for methanol oxidation was also tested. The nanorods grown in a membrane of 18 mm of diameter were dispersed, after the etching of the membrane and exhaustive cleaning, in 1ml of ethanol absolute and 7 µl of the dispersion deposited on a glassy carbon electrode of 2 mm of diameter. Therefore, the loading of catalysts on the support (glassy carbon) was of 1.8 µg. Figure 5 shows the

tested nanorods and the corresponding methanol electro-oxidation response. Unlike the films, significant differences in the surface morphology of the two types of nanorods are not observed. The geometrical area of the deposited nanorods has been calculated taking into account the membrane porosity (4.18%, specified by the supplier), the measured average diameter of the nanorods (125 nm) and their measured average length (2.75 μm), resulting a geometric area of 0.067 cm^2. However, the effective area is, probably, lower due to the agglomeration of some nanorods as a consequence of the magnetic attraction between them. As it has been found for the films tested, the methanol electro-oxidation is slightly more favourable on the Co_7Ni_3 nanorods of mainly hcp phase than on the Co_6Ni_4 ones with hcp+fcc mixed phase. In the case of the nanorods, the improved performance cannot be attributed at the surface texture or morphology because this seems to be almost the same. This result seems to be against the published in previous works [29-32], although no one compare alloys of different crystalline phase and similar composition. Different authors propose that CoNi films with increasing nickel percentage improve the methanol oxidation [29-31]. In our case, slightly better performance has been observed for the Co_7Ni_3 nanorods than for the Co_6Ni_4 ones, which suggests a higher activity the surface of the nanorods with hcp phase. Therefore, the control of the crystalline structure in the catalyst for methanol oxidation can be an important factor to improve their performance.

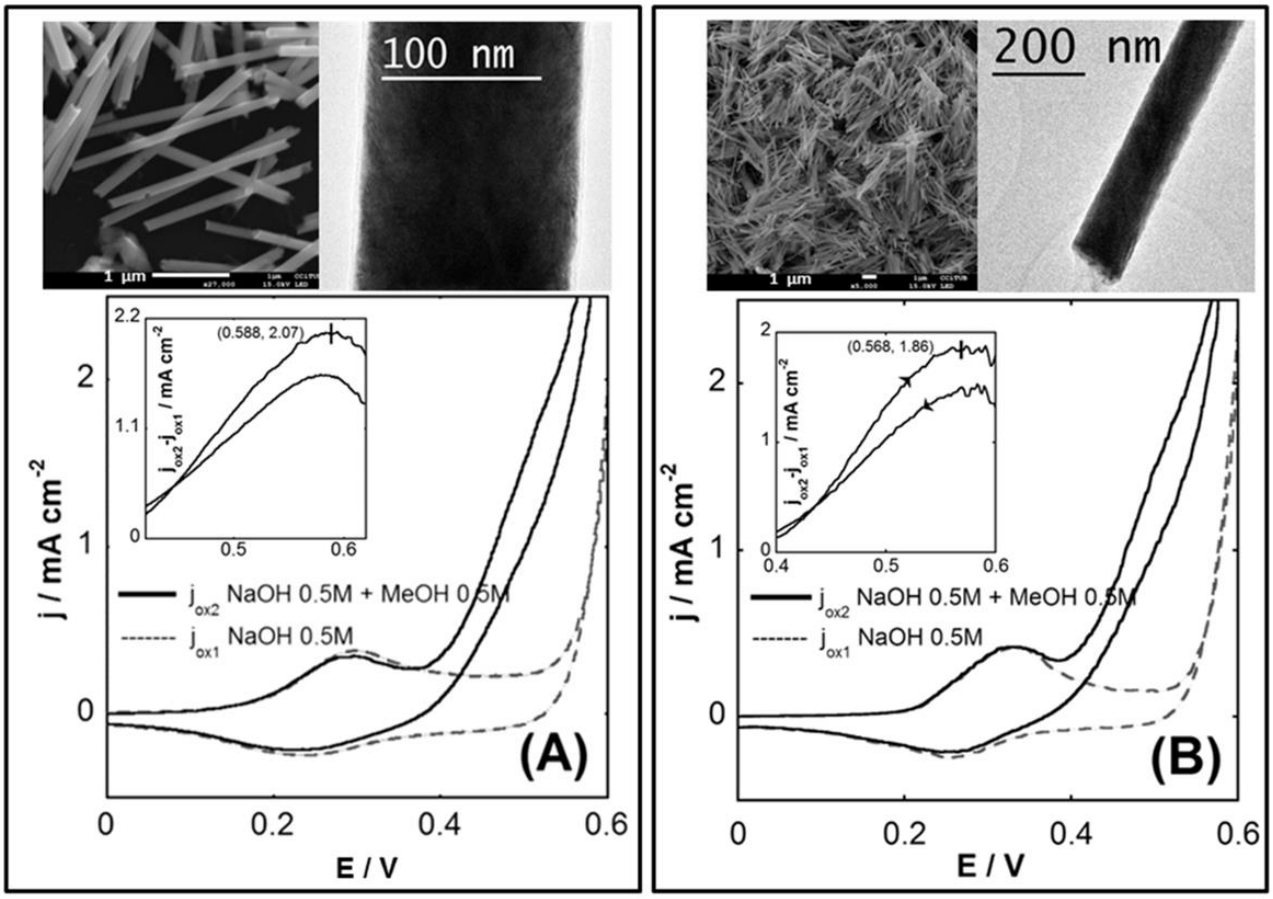

Figure 5

4.-Conclusions

We have electrochemically synthesised, from a single electrolytic bath, CoNi nanorods of similar composition (Co_7Ni_3 and Co_6Ni_4) but different crystalline structure (main hcp and hcp+fcc, respectively) by controlling the deposition potential. These nanorods maintain uniform composition and crystalline structure during their growth, from 1 to 10 µm length. Therefore, nanorods of defined properties, independent of their length, can be potentiostatically synthesised. The deposition potential controls the transport properties of the Co(II) and Ni(II) electroactive species and, then, the deposition rate, the composition and the crystalline structure. The CoNi nanorods synthesised have been tested as possible catalysts for methanol electro-oxidation, by analysing the behaviour of nanorods of similar composition but different crystalline structure. For the same geometrical area, the activity of the nanorods is almost the double than of the films. Moreover, the nanorods show better activity as catalyst with a very small volume and metal amount. To obtain the same area of catalyst (CoNi) in the form of films (1 micron thick) it is necessary a loading of around 30 times

more than for the synthesised nanorods. CoNi nanorods are therefore promising catalysts for methanol oxidation in basic medium.

The influence of the crystalline structure of CoNi films and nanorods of similar composition has been detected. The higher activity of Co_7Ni_3 over the Co_6Ni_4 both films and nanorods in spite of the reduction in a 25% of the more active nickel metal suggests a more superficial activity of the hcp phase over the fcc one, as well as than the increase in the effective area of the hcp structure in the case of the films.

Acknowledgements

MINECO contract CTQ2010-20726 (BQU subprogram) financed the work. The authors wish to thank the Centres Científics I Tecnològics de la Universitat de Barcelona (CCiTUB) for the use of their equipment and the Instituto de Microelectrónica de Barcelona (CNM-CSIC) for the Si/Ti/Au substrates supply.

References:

[1] E. Gómez, J. Ramírez, E. Vallés, *J. Appl. Elctrochem.* 28 (1997) 71-79

[2] N. Zech, E.J. Podlaha, D. landot. *J. Electrochem. Soc.* 14 (1999) 2886-2891

[3] E. Gómez, E. Vallés, *J. Appl. Electrochem.* 29 (1999) 805-812

[4] C. Lupi, D. Pilone, *Miner. Eng.* 14(11) (2001) 1403-1410

[5] L. Burzynska, E. Rudnik, *Hydrometallurgy* 54 (2000) 133-149

[6] A. Dolati, M. Sabati, N. Nouri, M. Ghorbani, *Mater. Chem. Phys.* 102 (2007) 118-124

[7] Y. Li, H. Jiang, W. Huang, H. Tian, *Appl. Surf. Sci.* 254 (2008) 6865-6869

[8] Y-F. Yang, B. Deng, Z-H. Wen, *Adv. Chem. Eng. Sci.* 1 (2011) 27-32

[9] C. Lupi, A. Dell'Era, M. Pasquali, P. Imperatori, *Surf. Coat. Technol.* 205 (2011) 5394-5399

[10] L. Tian, J. Xu, S. Xiao, *Vacuum* 86 (2011) 27-33

[11] L. Tian, J. Xu, C. Qiang, *Appl. Surf. Sci.* 257 (2011) 4689-4694

[12] L. Wang, Y. Gao, T. Xu, Q. Xue, *Mater. Chem. Phys.* 99 (2006) 96-103

[13] L. Wang, Y. Gao, Q. Xue, H. Lui, T. Xu, *Appl. Surf. Sci.* 242 (2005) 326-332

[14] M. Srivastava, V.E. Selvi, V.K. William, K.S. Rajam, *Surf. Coat. Technol.* 201 (2006) 3051-3060

[15] M.P. Proenca, C.T. Sousa, J. Ventura, M. Vázquez, J. Araujo, *Nanoscale Res. Lett.* 7 (2012) 280, 9pp.

[16] V.M. Prida, J. Garcia, L. Iglesias, V. Vega, D. Görlitz, K. Nielsch, E. Diaz, R. Mendoza, A. Ponce, C. Luna, *Nanoscale Res. Lett.* 9 (2013) 263, 7pp.

[17] M.Y. Rafique, L. Pan, W.S. Khan, M.Z. Iqbal, H. Qiu, M.H. Farooq, M. Ellahi, Z. Guo, *CrysEngCom.* 15 (2013) 5314-5325

[18] S. Talatrapa, X. Tang, M. Padi, T. Kim, R. Vajtai, G.V.S. Sastry, M. Shima, S.C. Deevi, P.M. Ajayan, *J. Mater. Sci.* 44 (2009) 2271-2275

[19] A. Ghahremaninezhada, A. Dolati, *J. Alloy Compd.* 480 (2009) 275-278

[20] A. Pereira, C. Gallardo, A.P. Espejo, J. Briones, L.G. Vivas, M. Vázquez, J.C. Denardin, J. Escrig, *J. Nanopart. Res.* 15 (2013) 2041, 8pp

[21] K.R. Pirota, F. Béron, D. Zanchet, T.C.R. Rocha, D. Navas, J. Torrejón, M. Vázquez, M. Knobel, *J. Appl. Phys.* 109 (2011) 083919

[22] V. Vega, T. Bohnert, S. Martens, M. Waleczek, J.M. Montero, D. Gorlitz, V.M. Prida, K. Nielsch, *Nanotechnology* 23 (2012) 465709, 10pp.

[23] L.G. Vivas, M. Vázquez, J. Escrig, S. Allende, D. Altbir, D.C. Leitao, J.P. Araujo, *Physical Review B* 85 (2012) 035439, 8pp

[24] J. Vilana, E. Gómez, E. Vallés, *J. Electroanal. Chem.* 703 (2013) 86-96

[25] F. Wolfart, A.L. Lorenzen, N. Nagata, M. Vodotti, *Sens. Actuat. B.* 186 (2013) 528-535

[26] C. Gonzalez-Buch, I. Herraiz-Cardona, E. Ortega, J. García-Antón, V. Perez-Herranz, *Int. J. Hydrogen Energ.* 38 (2013) 10157-10169

[27] C. Lupi, A.Dell'Era, M. Pasquali. *Int. J. Hydrogen Energ*. 34 (2009) 2001-2006

[28] S.H. Hong, S.H. Ahn, I. Choi, S.G. Pyo, H-J. Kim, J.H. Jang, S-K. Kim, *Appl. Surf. Sci.* 307 (2014) 146-152

[29] A.M.N. Barakat, M. Motlak, B-. Kima, A.G. El-Deen, S.S. Al-Deyabe, A.M. Hamza, *J. Mol. Catal. A- Chem* 394 (2014) 177-187

[30] X. Tarrús, M. Montiel, E. Vallés, E. Gómez, *Int. J. Hydogen Energ*. 39 (2014) 6705-6713

[31] Xun Cui, Wenlong Gao, Ming Zhou, Yang Yang, Yanhui Li, Peng Xiao, Yun-huai Zhang, Xiaoxing Zhang, *ACS Appl. Mater. Inter*. 7 (2015) 493-503.

[32] A.M.N. Barakat, M. Motlak, A.A. Elzatahry, K.A. Kahil, E.A.M. Abdelghani, *Int. J. Hydrogen Energ.* 39 (2014) 305-316

[33] N. Motoyama, Y. Fukunaka, T. Sakka, Y.H. Ogata, *Electrochim. Acta* 53 (2007) 205-212.

[34] D.A. Bograchev, V.M. Volgin, A.D. Davydov, *Electrochim. Acta* 96 (2013) 1– 7

Captions for figures

Figure 1.-Evolution of the intensity during the growth of CoNi nanrods in the interior of the nanochannels of a gold coated polycarbonate membrane, at two deposition potentials applied. Detail inside: zoom of the initial part of the curves

Figure 2.-SEM images of the CoNi nanorods obtained at different times for two potentials applied and dependence of the average length of the nanorods as a function of the deposition time

Figure 3.-TEM representative images of some CoNi nanorods and Selected Area Diffraction (SAED) Patterns of the different zones of the nanorods obtained at two deposition potentials

Figure 4.-SEM pictures of Co_7Ni_3 hcp film (A) and Co_6Ni_4 fcc film (B) synthesised respectively at -800 mV and -1000 mV. Cyclic voltammograms of a 0.5 M NaOH solution (dotted line) and 0.5 M NaOH+0.5 MeOH solution (continuous line) on the Si/Ti/Au/Co_7Ni_3 (A) and Si/Ti/Au/Co_6Ni_4 (B) substrates. 50 mV s^{-1}. Cycle number 30. Thickness of the CoNi deposits: 1 μm

Figure 5.-SEM and TEM images of the Co_7Ni_3 hcp nanorods (A) and Co_6Ni_4 hcp+fcc nanorods (B) synthesised at -800 and -1000 mV, respectively. Cyclic voltammograms of a 0.5 M NaOH solution (dotted line) and 0.5 M NaOH+0.5 MeOH solution (continuous line) on the glassy carbon/Co_7Ni_3 nanorods (A) and glassy carbon/Co_6Ni_4 nanorods (B). 50 mV s^{-1}. Cycle number 30. Length of the nanorods: 2.75 μm.